A Force-Controllable Compact Actuator Module for a Wearable Hand Exoskeleton ⋆

Inseong Jo and Joonbum Bae∗

Bio-Robotics and Control (BiRC) Laboratory,
School of Mechanical and Nuclear Engineering, UNIST,
Ulsan, Korea, (e-mail: {isjo, jbbae}@unist.ac.kr)

Abstract: In this paper, a force-controllable compact actuator module for a wearable hand exoskeleton system is proposed. To interact with virtual objects naturally with a hand exoskeleton, a small actuator module, which can generate the desired force accurately, is highly required. In the proposed actuator module, a series elastic actuator (SEA) mechanism was applied for the force mode control. Based on the experimental analysis about grip forces, a spring was manually designed and a linear motor was selected. A manually designed motor driver was also embedded to the actuator module. The actually manufactured actuator module was compact enough to put five modules at the back of the hand. For precise force mode control, friction of the motor was identified and compensated. Using a PID controller with the friction compensation, the proposed actuator module could generate the desired force accurately with actual finger movements.

Keywords: Hand exoskeleton system, Virtual reality, Force mode control, Series elastic actuator

1. INTRODUCTION

Exoskeleton systems have been actively researched for rehabilitation, power augmentation, and so on (Zoss et al. [2006], Riener et al. [2005], Veneman et al. [2007], Perry et al. [2007]). Among the research areas, interacting with virtual objects using an exoskeleton interface is one of the most promising applications of the exoskeleton systems. Many related researches to achieve the virtual reality such as head mounted display (HMD) systems or tactile sensors are also actively researched (OculusVR [2013], SONY [2013], Jonathan Engel and Liu [2003]), which accelerates the needs of a wearable interaction system for the hand.

Since the hand is the richest source of tactile feedback, delicate interaction with virtual objects may not be possible without appropriate force feedback to the hand. To develop a wearable interaction system for the virtual reality, the system should be able to deliver the desired interactive force from virtual objects accurately to the user while guaranteeing natural motions of fingers. In our previous research, we have selected the exoskeleton structure as a wearable interaction system for the hand because of its force delivering ability to the fingertip, and designed the exoskeleton structure based on the hand anatomy (Jo and Bae [2013]). In this paper, a compact actuator module, which is able to generate and control the desired force precisely, is proposed.

A small and force-controllable actuator module is highly required for the hand exoskeleton system. Because the

actuator modules mainly determine the size and weight of the system, which has a great effect on the natural motions of the arm and fingers, the actuator module should be small and light as much as possible. Also, when a user interacts with objects in the virtual world, the user understands the virtual surroundings and manipulates objects based on the transmitted force information. Thus, the force feedback is important in the hand exoskeleton system. For force mode control, a force sensor may be applied to the hand exoskeleton system, but a conventional force sensor is so large and heavy that it increases the size and weight of the system. In this paper, series elastic actuator (SEA) mechanism with an electric motor is applied to the actuator module to satisfy both requirements: compact size and force mode control. In the SEA mechanism, the transmitted force is measured by the spring deflection between the actuator and the human side. The spring acts as a force sensor, thus the size and weight of the actuator module can be reduced. By adjusting the actuator position, the transmitted force is accurately controlled.

This paper is organized as follows. In section 2, previously developed actuators for the hand exoskeleton systems are reviewed, and design of the actuator module is proposed. The control algorithm of the actuator module for accurate force mode control is discussed and verified by experiments in section 3. The performance of the actuator module with the actual hand exoskeleton is verified by experiments in section 4. Conclusions and future works are given in section 5.
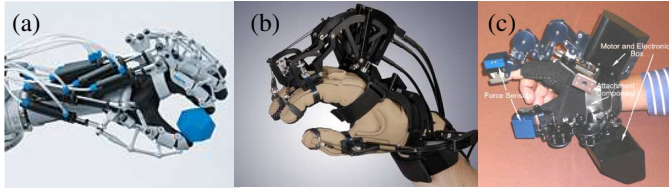
Fig. 1. Previously developed hand exoskeleton systems

2. DESIGN OF THE ACTUATOR MODULE

2.1 Previously Developed Actuator Modules

There have been a lot of attempts to develop actuator modules for wearable hand exoskeleton systems. For the actuating system of hand exoskeletons, pneumatic actuators or electric motors were usually applied. Exo-Hand by FESTO in Fig. 1(a) used pneumatic actuators as the actuating system (FESTO [2013]). The pneumatic actuator has the highest power density than other actuating systems, but the required extra equipment such as pump and valve systems restricts its mobility.

Figures 1(b) and (c) show the hand exoskeleton systems using electric motors. Cyber Grasp in Fig. 1(b) was developed as a cable-driven system using one electric motor to each finger (Cyber Glove Systems [2013]). Only one actuator is used for each finger, but the whole system is quite bulky due to the cable transmission mechanism. The hand exoskeleton developed by PERCRO shown in Fig. 1(c) has three motors for each finger to change the direction and magnitude of the applied force (Fontana et al. [2009]). Due to the many actuators, three directional forces can be generated, but it is too large and heavy for the arm and finger to be moved naturally.

Since the previously developed actuator modules did not have force sensors, the interactive force could not be accurately controlled even some of them were force-controllable in open loop. Thus, the compact and force-controllable actuator module for delicate interaction with virtual objects has not been developed yet.

2.2 Series Elastic Actuator (SEA) Mechanism

To apply accurate force feeling to the finger, force mode control is required, which needs real-time force measurement. However, a conventional force sensor may not be appropriate for the hand exoskeleton system due to its bulky size and heavy weight. In the proposed hand exoskeleton system, a series elastic actuator (SEA) mechanism is applied for the compact design and accurate force mode control.

The SEA mechanism has been widely used for the physical human-robot interaction systems for force mode control (Pratt et al. [2002], Paluska and Herr [2006], Pratt and Williamson [1995], Bae et al. [2011, 2013], Bae and Tomizuka [2012]). In this mechanism, the force generated by an actuator is transmitted via the elastic element, i.e., a spring, which is installed between the human side and the actuator. The transmitted force is controlled by the spring deflection. The schematic of the SEA mechanism is shown in Fig. 2. The transmitted force, f, is controlled by the deflection of the spring as follows:
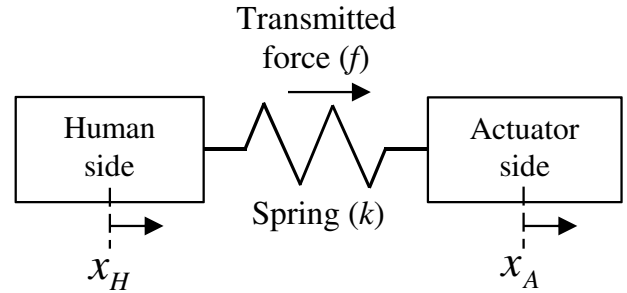

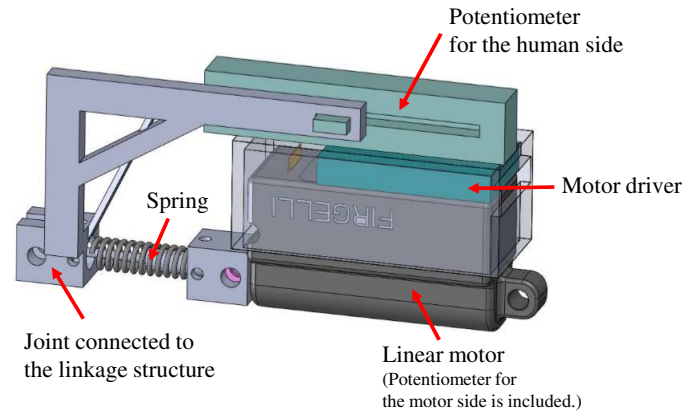Fig. 2. Schematic of the series elastic actuator (SEA) mechanism

Fig. 3. Design of the actuator module

$$f = k(x_A - x_H) \tag{1}$$

where k is the spring constant, x_A and x_H are positions of the actuator and human side, respectively. The desired actuator position is determined by the measured human joint motion and the given desired force, f_d, as follows:

$$x_{Ad} = \frac{f_d}{k} + x_H \tag{2}$$

where x_{Ad} is the desired actuator position. By controlling the motor position, the desired force can be generated accurately; thus, the actuator can interact with the human motion by applying appropriate interactive force by (1).

In the proposed hand exoskeleton system, the SEA mechanism is applied to implement a force-controllable actuator module. The Solidworks design of the actuator module is shown in Fig. 3. The position of a finger linkage structure is measured by the potentiometer for the human side, and that of an actuator is measured by the embedded potentiometer in the linear motor. The transmitted force is controlled by the deflection of the linear spring.

Because the transmitted force is applied and measured using the linear spring deflection, the hand exoskeleton system does not require a force sensor. This mechanism makes the design of actuator module compact, and the sensitivity of measuring force is easily adjusted by the spring constant.

2.3 Design of a Linear Spring

The linear spring plays a very important role in the proposed force-controllable actuator module because the force is transmitted through the spring. Thus, the spring

Table 1. Parameters of the spring design

Modulus of rigidity	G (kgf/mm^2)	7500
Diameter of a spring wire	d (mm)	0.6
Mean diameter of a spring	D (mm)	6.5
Number of turns	n	10
Spring constant	k (N/mm)	0.434

constant should be carefully determined because maximum force and sensitivity of the actuator module are determined by the spring constant.

The actuator module should be able to generate the maximum grip force to apply any amount of interactive forces from virtual objects to the fingers. The grip forces were experimentally measured by Tekscan Grip sensor (Tekscan [2013]) shown in Fig. 4(a). Seven healthy persons (four males, three females, age: 24±4.3) were participated in measuring grip forces. They were asked to grip a solid plastic cup with size of 6.4 cm diameter smoothly for 30 seconds. Each person had the test for five times. The average grip forces of each finger were calculated for male and female participants. The experimental results are shown in Fig. 4(b). The grip force of the thumb was largest for all participants, which are about 8 N for males and about 6 N for females.

In our previous work, we designed the linkage structure of the hand exoskeleton system whose fingertip can be moved by the actuator installed at the back of the hand (Jo and Bae [2013]). Also, the simulation results showed that the fingertip could be flexed to 80 deg and hyper-extended to 30 deg with about 25 deg actuator link motion. With the previously designed exoskeletal structure and actuator module in Fig. 3, it was verified that the 25 deg rotation motion could be achieved by about 20 mm linear motion of the actuator. Thus, the linear motor with stroke of about 20 mm is necessary, which can make maximum 20 mm deflection. Considering the maximum force and deflection, the required spring constant is about 0.3~0.4 N/mm.

The spring constant is calculated as follows (Budynas and Nisbett [2011]):

$$k = \frac{Gd^4}{8D^3n} \tag{3}$$

where G is the modulus of rigidity, d is the diameter of a spring wire, D is the mean diameter of a spring, and n is the number of active coils. Considering the size of the linkage structure and the linear motor, the design parameters were determined to make the spring constant 0.434 N/mm. The determined variables for spring design are listed in Table 1.

2.4 Design of the Motor Driver

The motor driver to control the linear motor should also be compact enough to fit with the small actuator module. The motor driver for the linear motor was manually designed as shown in Fig. 5. Fig. 5(a) shows the circuit design for the actuator, and Fig. 5(b) is the actually manufactured motor driver. The control input to the motor driver is converted to a PWM signal and a full H bridge circuit is applied for normal/reverse motion of the electric motor. The size of the motor driver is $27 \times 14 \times 4$ mm, which is small enough to attach at the top of the linear motor.

(a) Tekscan Grip sensor
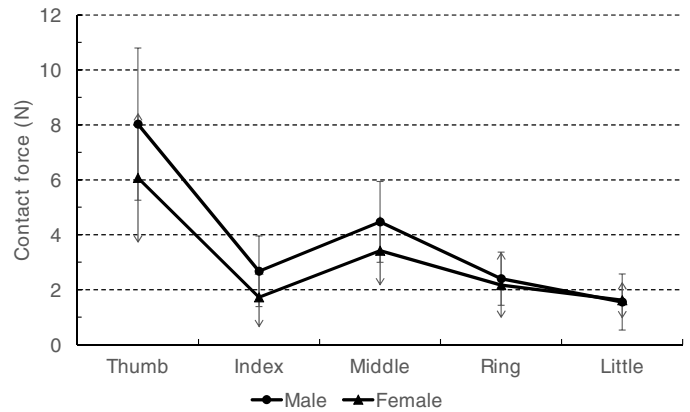
(b) Grip force distribution of each finger

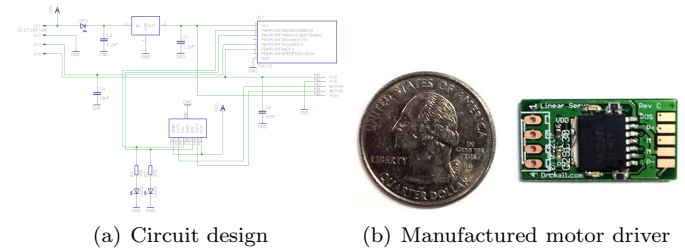Fig. 4. Experimental results on grip force

(a) Circuit design   (b) Manufactured motor driver

Fig. 5. Small size motor driver

2.5 The manufactured actuator module

The force-controllable actuator module was actually manufactured as shown in Fig. 6. To satisfy the required force and stroke range, a linear motor with 20 mm stroke, 9 N maximum force and 25 mm/sec speed was selected as a main actuator (Firgelli [2013]). The linear spring designed by the parameters in Table 1 was applied. The potentiometer to measure the finger motion was placed to the top of the actuator module because of the limited space. The motor driver was attached to the top of the motor and hidden by a manufactured cover to protect electronic lines. The structure was manufactured with nylon material using a rapid prototyping technology. The size of the actuator module is about $18 \times 77 \times 36$ mm, and the weight is about 30 g.
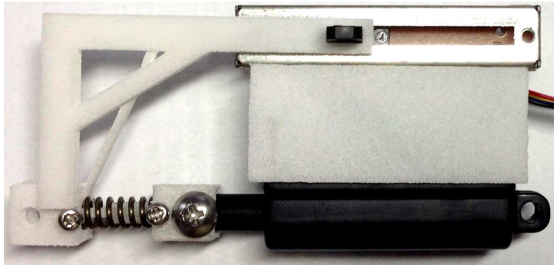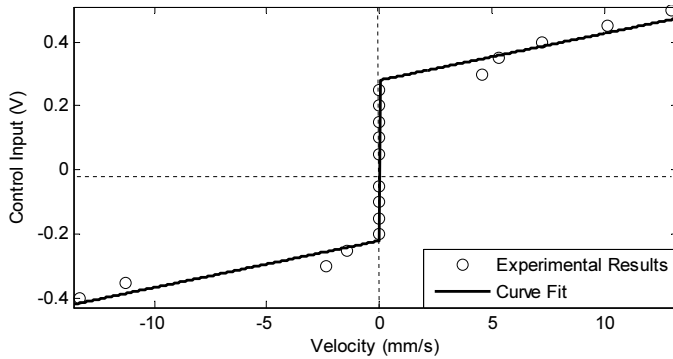
Fig. 6. Manufactured actuator module

Fig. 7. Friction identification

3. CONTROL OF THE ACTUATOR MODULE

3.1 Control Algorithm with Friction Compensation

An electric motor is usually used with a gear reducer to adjust the force or speed range as desired. The gear reducer amplifies the output force, but it also amplifies friction of the motor. If the gear ratio is so large that the geared motor is not back-drivable, then the friction should be appropriately compensated for natural human-robot interaction. Since the friction in the motor is the dominant nonlinearity which prohibits high control performance in position tracking, the force-controlled ability of the proposed actuator module is significantly decreased without appropriate friction compensation.

In the proposed actuator module, a linear motor with gear ratio 30:1 was used, thus friction of the motor is not negligible. To compensate friction of the motor, the friction model was experimentally identified. Figure 7 shows the experimentally obtained control inputs at various velocities of the motor. Then, the friction is modeled by,

$$f = a + b \cdot sgn(v_A) + c \cdot v_A \qquad (4)$$

where v_A is the velocity of actuator. Each term in (4) represent bias, Coulomb friction, and linear damping, respectively. By curve fitting, the parameters in the friction model were identified as $a = 0.05$, $b = 0.2$, and $c = 0.003475$.

The linearized motor model by the friction compensation was controlled by a PID controller. The PID gains were tuned manually. Figure 8 shows the control block diagram of the actuator module.

The frequency response of the closed loop control system was experimentally obtained as shown in Fig. 9. In the experiment, sinusoidal signals with 5 mm magnitude and
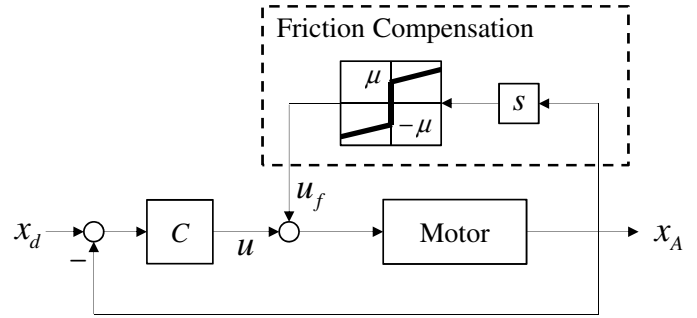

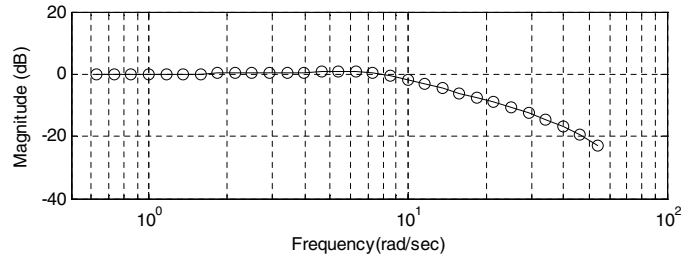Fig. 8. Block diagram of the control algorithm

Fig. 9. Frequency response of the closed loop control system

different frequency were swept. As shown in the figure, the bandwidth frequency of the actuator module is about 10 rad/sec. Considering the maximum speed of the linear motor, the experimental results show that the control algorithm guarantees the maximum performance of the motor.

### 3.2 Experimental Verification of the Control Algorithm

The position tracking performance with the proposed control algorithm was verified by experiments. Figure 10 shows the tracking performance of desired trajectory with a sinusoidal signal of 0.5 Hz frequency and 5 mm magnitude. The linear motor follows the desired trajectory within 0.5 mm error. In order to test the tracking performance for an arbitrary trajectory, the desired trajectory was set to the potentiometer signal of the human side, and it was moved arbitrary, Figure 11 shows the experimental result with an arbitrary desired trajectory. With the arbitrary motion, the tracking error is more irregular than that of the sinusoidal signal, but the tracking error is below 1 mm with about 10 mm change in the desired position.

4. PERFORMANCE VERIFICATION OF THE ACTUATOR MODULE WITH THE HAND EXOSKELETON

The proposed actuator modules were actually assembled with the hand exoskeleton structure proposed in (Jo and Bae [2013]). In this design, the generated force is delivered to the fingertip through the exoskeletal linkage. Also, the exoskeletal structure allows three degrees of freedom and enough extension/flexion movement to each finger for natural interaction with the hand. Figure 12(a) shows the 3D design of the hand exoskeleton system with the assembled actuator modules, and Fig. 12(b) shows the actually manufactured hand exoskeleton. Two actuator modules were installed for the experiments.
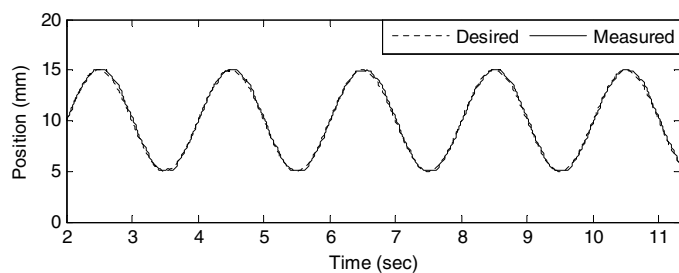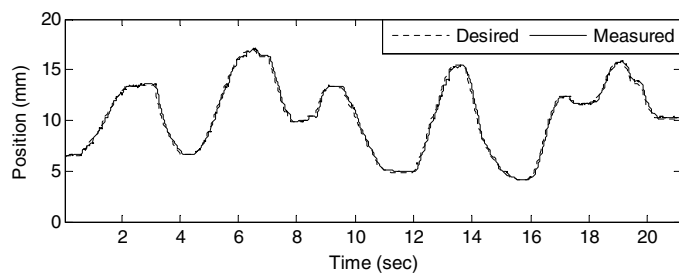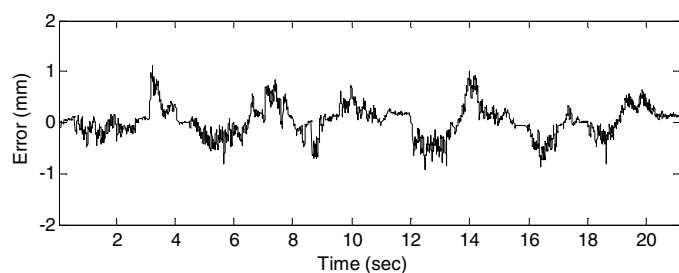
(a) Desired and measured position
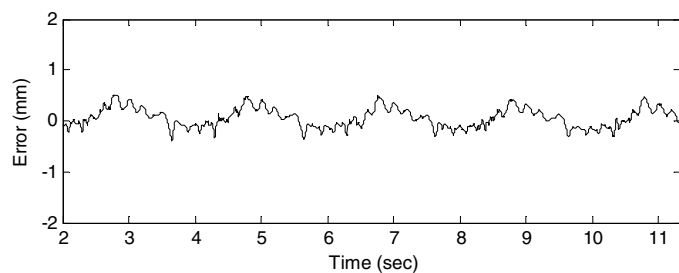
(b) Tracking error

Fig. 10. Position tracking with a sinusoidal desired trajectory

(a) Desired and measured position

(b) Tracking error

Fig. 11. Position tracking with an arbitrary desired trajectory

The force control performance with the actual exoskeleton structure was experimentally verified. In this experiment, the desired force was set to a sinusoidal signal with the frequency of 0.5 Hz and the amplitude of 5 N and the human side potentiometer moved along arbitrary motion of the finger. By using (2) and manually designed spring constant, the desired motor position (Fig. 13(a)) for force mode control was calculated in real time by the desired force and the finger position. Figure 13 shows the performance of desired force generation with arbitrary finger motion. Even with the arbitrary motion of the finger, the force is generated as desired with the error of about 0.5 N.
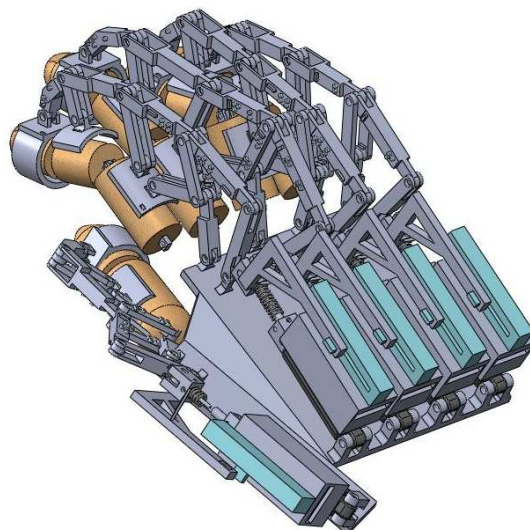
(a) 3D design of the hand exoskeleton

(b) Manufactured hand exoskeleton

Fig. 12. Hand exoskeleton with actuator modules

5. CONCLUSION

In this paper, a compact and force-controllable actuator module for a hand exoskeleton system was proposed and its performance was verified by experiments. To develop a compact and force-controllable actuator module, series elastic actuator (SEA) mechanism was applied. In this mechanism, the spring installed between the actuator and the exoskeleton frame acts as a force sensor, which reduces the size and weight of the actuator module and enables force mode control. The spring was manually designed considering the maximum grip force and required actuator stroke. For the control of the actuator module, the geared motor was linearized by friction compensation, and a PID controller was applied. The experimental results showed that the proposed actuator module could generate the desired force accurately with an arbitrary finger motion.

As the future work, the actuator module will be installed to all five fingers, and the applied forces to the fingertips from the actuator modules will be compared with actual interactive forces from real objects. With those data, actuator modules will be revised and upgraded.
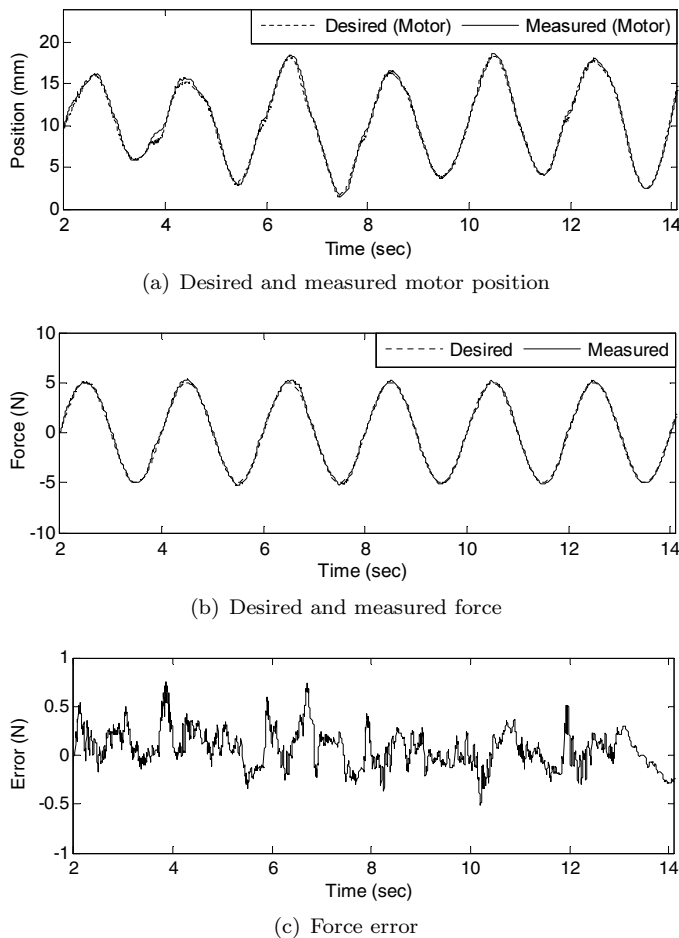
(a) Desired and measured motor position

(b) Desired and measured force

(c) Force error

Fig. 13. Force control with arbitrary finger motion

REFERENCES

J. Bae and M. Tomizuka. A gait rehabilitation strategy inspired by an iterative learning algorithm. *Mechatronics*, 22:213–221, 2012.

J. Bae, W. Zhang, and M. Tomizuka. Network-based rehabilitation system for improved mobility and tele-rehabilitation. *IEEE Transactions of Control Systems Technology*, 21:1980–1987, 2013.

Joonbum Bae, Kyoungchul Kong, and Masayoshi Tomizuka. Gait phase-based control for a rotary series elastic actuator assisting the knee joint. *ASME Journal of Medical Devices*, 5:031010–1–6, 2011.

Richard G. Budynas and J. Keith Nisbett. *Shigley's Mechanical Engineering Design*. McGraw-Hill, 2011.

Cyber Glove Systems. *Cyber Grasp*. 2013. URL http://www.cyberglovesystems.com/.

FESTO. *Exo-Hand*. 2013. URL http://www.festo.com/.

Firgelli. *PQ 12 Series*. 2013. URL http://www.firgelli.com/.

M. Fontana, A. Dettori, F. Salsedo, and M. Bergamasco. Mechanical design of a novel hand exoskeleton for accurate force displaying. *IEEE International Conference on Robotics and Automation (ICRA)*, pages 1704–1709, 2009.

Inseong Jo and Joonbum Bae. Kinematic analysis of a hand exoskeleton structure. *International Conference on Ubiquitous Robots and Ambient Intelligence (URAI)*, pages 457–458, 2013.

Jack Chen Jonathan Engel and Chang Liu. Development of polyimide fexible tactile sensor skin. *Joural of Micromechanics and Microengineering*, 13:359–366, 2003.

OculusVR. *Oculus Rift*. 2013. URL http://www.oculusvr.com/.

D. Paluska and H. Herr. Series elasticity and actuator power output. *IEEE International Conference on Robotics and Automation (ICRA)*, pages 1830–1833, 2006.

Joel C. Perry, Jacob Rosen, and Stephen Burns. Upper-limb powered exoskeleton design. *IEEE/ASME Trans. Mechatron.*, 12:408–417, 2007.

G.A. Pratt and M. Williamson. Series elastic actuators. *IEEE/RSJ Int. Conf. Intell. Robotics Syst. (IROS)*, pages 399–406, 1995.

J. Pratt, B. Krupp, and C. Morse. Series elastic actuators for high fidelity force control. *Int. J. Ind. Robot*, 29: 234–241, 2002.

R. Riener, L. Lunenburger, S. Jezernik, M. Anderschitz, G. Colombo, and V. Dietz. Patient-cooperative strategies for robot-aided treadmill training: first experimental results. *IEEE Trans. Neural Syst. Rehabil. Eng.*, 13: 380–394, 2005.

SONY. *3D Personal Viewer*. 2013. URL http://www.sony.com/.

Tekscan. *Grip System*. 2013. URL http://www.tekscan.com/.

Jan F. Veneman, Rik Kruidhof, Edsko E.G. Hekman, Ralf Ekkelenkamp, Edwin H.F. Van Asseldonk, and Herman van der Kooij. Design and Evaluation of the LOPES Exoskeleton Robot for Interactive Gait Rehabilitation. *IEEE Trans. on Neural System Rehabilitation Engineering*, 15:379–386, 2007.

A. Zoss, H. Kazerooni, and A. Chu. Biomechanical design of the berkeley lower extremity exoskeleton (BLEEX). *IEEE/ASME Trans. Mechatronics*, 11:128–138, 2006.